Proceedings of the ASME 2010 Eighth International Fuel Cell Science, Engineering and Technology Conference
FuelCell2010
June 14-16, 2010, Brooklyn, New York, USA

FuelCell2010-33308

EFFECTS OF GAS FLOW RATE AND CATALYST LOADING ON POLYMER ELECTROLYTE MEMBRANE (PEM) FUEL CELL PERFORMANCE AND DEGRADATION

A. Chukwujekwu Okafor and Hector-Martins Mogbo
Department of Mechanical and Aerospace Engineering
Missouri University of Science and Technology
327 Toomey Hall
Rolla, MO 65409-0050
Phone: 573-341-4695, Fax: 573-341-6899, E-mail: okafor@mst.edu

ABSTRACT

In this paper, the effects of gas flow rates, and catalyst loading on polymer electrolyte membrane fuel cell (PEMFC) performance was investigated using a 50cm² active area fuel cell fixture with serpentine flow field channels machined into poco graphite blocks. Membrane Electrode Assemblies (MEAs) with catalyst and gas flow rates at two levels each (0.5mg/cm², 1mg/cm²; 0.3L/min, 0.5L/min respectively) were tested at 60°C without humidification. The cell performance was analyzed by taking AC Impedance, TAFEL plot, open circuit voltage, and area specific resistance measurements. It was observed that MEAs with lower gas flow rate had lesser cell resistance compared to MEAs with a higher gas flow rate. TAFEL plot shows the highest exchange current density value of -2.05 mAcm² for MEA with 0.5mg/cm² catalyst loading operated at reactant gas flow rate of 0.3L/min signifying it had the least activation loss and fastest reaction rate. Open circuit voltage curve shows a higher output voltage and lesser voltage decay rate for MEAs tested at higher gas flow rates.

1. INTRODUCTION

Proton Exchange Membrane (PEM) fuel cells are being considered as one of the most promising emerging power generation technologies to take over from existing power generation technologies such as internal combustion engines in automotive applications. They are electrochemical devices that convert chemical energy of the reactants (hydrogen and oxygen) directly into electricity and heat with water as the only by-product. Figure 1 shows a schematic of a PEM Fuel Cell.

PEM Fuel Cells are highly efficient and have also gained interest as a clean alternative to many potential power source applications such as, stationary, transport, portable and micro power applications, as a result of their high power density, high efficiency, easily scalable modular construction, relatively safe and quiet operation, and low emission rate [1].

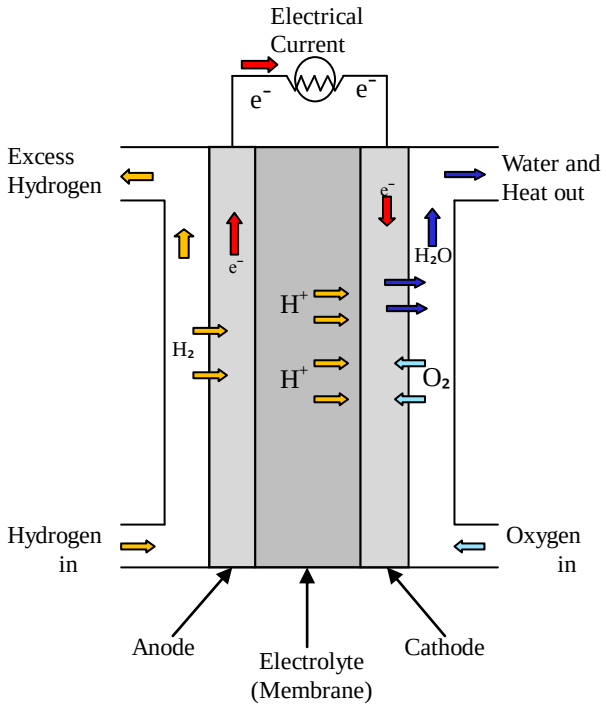

Figure 1. Schematic of a PEM Fuel Cell

However a lot of technical barriers are faced that prevent extensive commercialization of PEM fuel cells of which cost, performance and durability are the most important. All types of fuel cells exhibit a decrease in electrochemical performance with operation time, however, the degradation rates for different fuel cell types are different and depend strongly on operating conditions [2]. The presently high cost of PEM fuel cells need to be reduced to the target set by the US Department of Energy in order to compete with current market technologies including gasoline internal combustion engines. A lot of research is being done in order to reduce the cost of PEM fuel cells in a variety of ways including reducing the amount of platinum needed in each individual cell.

Another important barrier which hinders PEM fuel cell technology growth is the durability of the fuel cell under various operating conditions such as temperature, relative humidity (RH), etc. Stationary fuel cell applications require more than 40,000 hours of reliable operation, while automotive fuel cells require a life span of 5,000 hours of operation under extreme temperatures. Accordingly, there has been increased focus of study on fuel cell degradation issues by researchers and extensive studies are being carried out on membrane degradation mechanisms and failure in a fuel cell environment. For PEM fuel cells to meet the required lifetimes in various applications, the challenges posed by membrane degradation must be overcome. Performance degradation is unavoidable, but the degradation rate can be minimized through comprehensive understanding of degradation and failure mechanisms of each fuel cell component.

V. O. Mittal et al. showed that the main cause of membrane degradation is as a result of molecular H_2 and O_2 from reactant crossover through the membrane reacting on the surface of the Pt/C catalyst to form membrane degradation species [3]. The electrochemical performance of low temperature fuel cells degrades during operation and can be separated into reversible (recoverable after shut downs) and irreversible parts. The combination of electrochemical investigations of the electrodes and electrode-membrane-assemblies during the fuel cell operation with interface characterization by physical methods facilitates the identification of the important degradation processes. Different degradation processes are associated with reversible or irreversible performance degradation [4]. Membrane degradation are classified into mechanical, thermal, and electrochemical degradation, of which electrochemical degradation is the most severe and has the most effect on PEM fuel cell performance and durability[3, 5, 6].

Contamination of MEAs due to corrosion of cell assembly parts such as the bipolar plate, and gaskets/sealing materials can reduce the proton conductivity of the electrolyte and oxygen reduction kinetics at the cathode [7–9]. MEAs can be degraded by severe operating conditions such as insufficient flow of reactant gases [10, 11], change in humidification of the reactant gases, and change in operating temperature [12–13]. Improper water management may have detrimental effects on MEA degradation [14]. Delamination of the membrane and electrode is also a common means of failure in fuel cell membranes. This may be caused by differences in thermal and hydrated expansion properties of the different materials which cause delamination of different components of the PEMFC over time [15].

MEA catalyst degradation as a result of carbon support corrosion is another cause for concern in PEMFC performance and durability [16]. The platinum catalyst agglomerates during fuel cell operation and as a consequence, the active surface of the catalyst in the cathode decreases and the electrochemical performance decreases concurrently. This degradation is an irreversible process because the loss of surface area cannot be compensated by modification of the operating conditions [4]. More severely, chemical reaction on the anode and cathode catalysts can produce hydrogen peroxide which in turn produces radicals such as peroxide (OH) and hydro peroxide which are believed to be responsible for chemical attack on the membrane and catalyst [17]. Also the presence of trace metals such as Fe^{2+}, Fe^{3+}, and Cu^{2+} ions originating from bipolar plates and end plates can catalyze the reaction of radical formation leading to membrane thinning, formation of pinholes, and a chemical attack of the proton conducting end group, and back bone of the membrane material leading to PEMFC performance decay [18].

The mechanism of radical formation can be explained as shown in the following equations:

$$M^{2+} + H_2O_2 \rightarrow M^{3+} + OH + OH^- \quad (1)$$

$$M^{3+} + H_2O_2 \rightarrow M^{2+} + OOH + H^+ \quad (2)$$

$$C + H_2O_2 \rightarrow CO + H_2O \quad (3)$$

$$C + H_2O_2 \rightarrow HCOOH \quad (4)$$

Here, trace metal impurities in the membrane and electrodes such as Fe^{2+}, Cu^{2+} react with the hydrogen peroxide to form free radicals which go on to degrade the fuel cell components by reacting, and altering the membrane, electrode and catalyst compounds thereby leading to a fuel cell performance loss and eventual failure of the fuel cell [3, 19, 20].

The main objective of this paper is to investigate the effect of catalyst loading and reactant gas flow rate on Polymer Electrolyte Membrane (PEM) Fuel Cell performance and degradation using electrochemical testing methods, such as EIS, TAFEL plots, and OCV curve, and also to identify the degradation mechanisms and kinds of losses involved.

2. PEMFC PERFORMANCE ANALYSIS

2.1 Understanding Voltage Loss

Various disciplines of people are interested in fuel cells, and they have different terminology for similar ideas, especially in the field of engineering. Therefore it is very important that the language, as well as the engineering system be understood. One area that offers the most confusion is the topic of voltage differentials. The necessary term describing the voltage difference is “over-voltage” or “over-potential”. This term is most likely used by chemical and electrochemical engineers

and simply means the difference between the electrode potential and the equilibrium potential. The term "over-potential" has the same physical meaning with "voltage losses" which is the term electrical and mechanical engineers prefer to use. From the electrochemical engineers point of view, the difference between the electrode potential and the equilibrium potential is the driver for the electrochemical reaction, while from the mechanical or electrical engineer's point of view, it represents the loss of voltage and power.

When a fuel cell is supplied with the reactant gases needed for reaction, and for the fuel cell to operate, but the electrical circuit is open (Figure 2-1a), no current will be generated. As a result of this, it will be expected that the cell potential will be at, or close to, the theoretical cell potential of a fuel cell for given conditions i.e. temperature, pressure, and reactant gas concentration. Nevertheless, practically, this potential called the open circuit potential is significantly lower than the theoretical potential, usually less than 1V. This means there are some losses in the fuel cell even when no external current is generated. When the external current is closed (Figure 2-1b) with a load in it, the potential is expected to drop even further because of the current being generated, due to unavoidable losses. The different kinds of voltage losses in a fuel cell are caused by:

- kinetics of the electrochemical reaction
- internal electrical and ionic resistance
- difficulties in getting the reactants to the reaction sites
- internal (stray) currents
- crossover of reactants

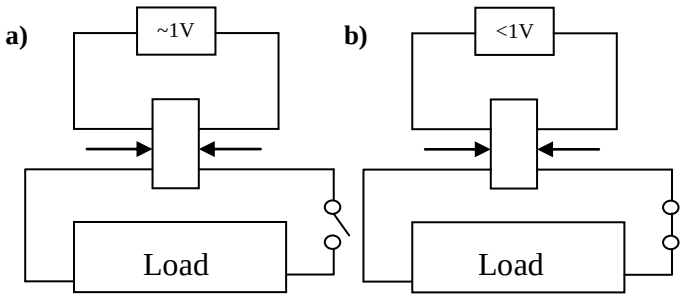

Figure 2-1: Fuel cell with load: a) in open circuit; b) load connected

These losses listed above can be broken down into three different types of losses. They are activation losses, internal currents and fuel crossover losses, and ohmic losses. Each of these losses has different effects on the theoretical voltage of the fuel cell thereby reducing its value [27, 28].

2.1.1 Activation Losses

The activation loss occurs because the chemical process initially has not begun, and it is associated with sluggish electrode kinetics [21]. Thus activation energy is necessary to insure that the reaction tends towards completion, which is forcing the hydrogen atoms to split into protons and electrons, and for the protons to travel through the electrolyte, and then combine with the oxygen and returning electrons. This loss is often termed over-potential, and is essentially the voltage difference between two terminals. Through experimentation, Tafel was able to mathematically and graphically describe these losses.

Figure 2-2 is known as a 'Tafel plot' and it shows that if a graph of overvoltage against *log* of current density is plotted, then for most values of the overvoltage, the graph approximates to a straight line. It relates the rate of an electrochemical reaction to the over potential. It also provides information about the mechanism, and the rate constant of the reaction taking place in a fuel cell. The exchange current density (i_o) value which can be obtained from the intercept of the best fit line on the current density axis is used to analyze the cell performance in terms of reaction rate.

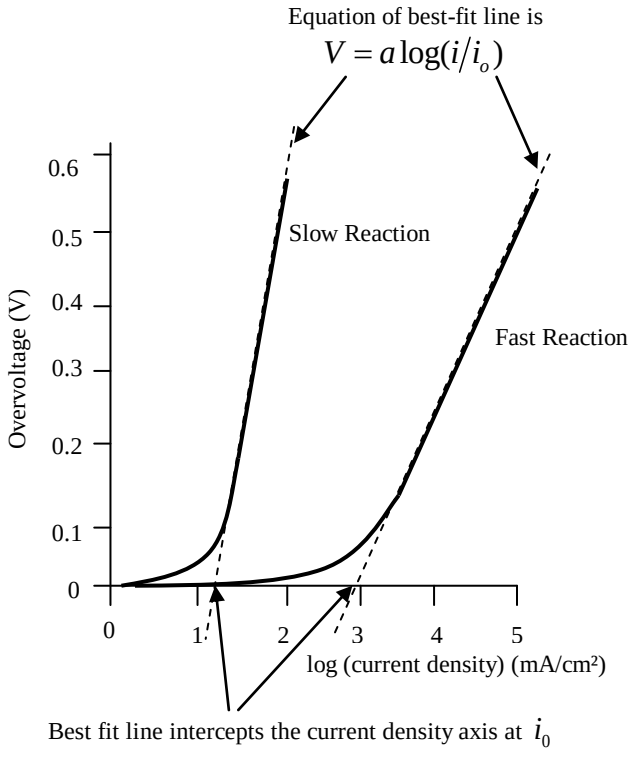

Figure 2-2: Tafel plots for slow and fast electrochemical reactions

The diagram shows two typical plots, and for most values of overvoltage its value is given by the equation:

$$\Delta V_{act} = a\log\left(\frac{i}{i_o}\right) \tag{2.1}$$

This equation is known as the Tafel equation, and can be expressed in many forms. To simplify the analysis, the equation is expressed in natural logarithm instead of base 10 as given in equation 2.2. Tafel equation 2.2 which is plotted in fig 2.2 shows Tafel plots for slow and fast electrochemical reactions.

$$\Delta V_{act} = A\ln\left(\frac{i}{i_o}\right) \tag{2.2}$$

The constant 'A' is higher for an electrochemical reaction that is slow, and the constant i_o is higher for faster reaction. The current density i_o which is usually called the exchange current density can be considered as the current density at which the over-voltage begins to move from zero. This exchange current density i_o is crucial in controlling the performance of a fuel cell electrode. A in equation (2.2) above is given by:

$$A = \frac{RT}{2\alpha F} \tag{2.3}$$

Where,
R = universal gas constant in ideal gas law
T = temperature in Kelvin
F = Faradays constant
α = charge transfer coefficient

The value α is described as the proportion of the electrical energy that is harnessed in changing the rate of an electrochemical reaction, and must be in the range 0 to 1.0 [27, 28].

To reduce activation losses and improve fuel cell performance, it is important to increase the value of i_o. This can be done in the following ways:

- by raising cell temperature
- using more effective catalysts
- increasing electrode roughness to increase reaction sites surface area
- increasing reactant concentration
- increasing pressure

2.1.2 Internal Currents and Fuel Crossover Losses

Although the electrolyte of a fuel cell is not electrically conductive, and is practically impermeable to reactant gases, some small amount of reactant gas, mainly hydrogen, will diffuse to the other side of the electrode, and some small amount of electron conduction will take place. This small amount of hydrogen that migrates through the electrolyte is known as fuel crossover, and the small amount of electrons that find a shortcut through the electrolyte is known as internal current. Because each hydrogen molecule contains two electrons, this fuel crossover and internal currents are essentially equivalent; The crossing over of one hydrogen molecule from the anode through the electrolyte to the cathode where it reacts, wasting two electrons, is exactly the same as two electrons crossing from the anode through the electrolyte to the cathode internally, rather than as an external current. These losses may appear insignificant in fuel cell operation because of the rate of hydrogen and electron crossover is several orders of magnitude lower than the hydrogen consumption rate or total electrical current generated. However, when the fuel cell is operated at open circuit potential or when it operates at very low densities, theses losses may have a very significant effect on cell potential. Since in both of these processes, two electrons are wasted, and prevented from travelling externally, the losses are similar in source and the same in result. This phenomenon can be modeled by modifying the Tafel equation in (2.2):

$$V = A\ln\left(\frac{i + i_n}{i_o}\right) \tag{2.4}$$

This modification will allow for the term i_n in the Tafel equation and will now account for the initial losses of voltage in low temperature fuel cells. It is not prevalent in high temperature fuel cells because the small value of i_n does not significantly change the ratio in the natural logarithm [27, 28].

2.1.3 Ohmic Losses

Voltage loss caused by ohmic resistance results mainly from resistance to the flow of ions in the electrolyte, and resistance to the flow of electrons through the electrode [22]. In most fuel cells the resistance is mainly caused by the electrolyte, though the electrodes can also be important. Ohmic losses are in standard ohmic form but are usually written in terms of current density and area specific resistance. This allows for the ease of use in evaluating performance of the cell. The equation for the voltage loss now becomes:

$$\Delta V_{ohm} = ir \tag{2.5}$$

Where,
i = current density in mA/cm²
r = area specific resistance in Ωcm²

As seen in equation (2.5), an increase in current density or area specific resistance increases ohmic loss. Thus to reduce ohmic loss it is necessary to use electrodes with extremely high conductivities, well designed bipolar plates, and thin electrolytes [27, 28].

2.2 AC Impedance Spectroscopy

AC Impedance/Electrochemical Impedance spectroscopy (EIS) is a powerful diagnostic tool that can be used to characterize limitations and improve the performance of a fuel cell. The EIS measurements allow to separate the losses of the electrochemical performance and to distinguish between the degradation processes taking place in the fuel cell components

[4]. The main advantage of EIS as a diagnostic tool for evaluating fuel cell behavior is its ability to resolve, in the frequency domain, the individual contributions of the various factors determining the overall PEM fuel cell power losses: ohmic, kinetic, and mass transport. Such a separation provides useful information both for optimization of the fuel cell design and selection of the most appropriate operating conditions [22]. In this method, an AC signal of known amplitude and frequency is sent through the cell, and the phase change and amplitude of the response is recorded. This may be repeated at different frequencies i.e. through an entire frequency spectrum. A common usage of EIS analysis in PEM fuel cells is to study oxygen reduction reaction (ORR) [23], to characterize transport (diffusion) losses [24], to evaluate ohmic resistance and electrode properties such as charge transfer resistance, double-layer capacitance, and to evaluate and optimize the membrane electrode assembly (MEA) [25, 26]. Impedance spectra are conventionally plotted in both Bode and Nyquist form. In a Bode plot, the amplitude and phase of the impedance is plotted as a function of frequency, while in a Nyquist plot the imaginary part of the impedance is plotted against the real part at each frequency.

With known amplitude and frequency, a signal is defined as:

$$I = I_{\max} \sin \ \omega t \tag{2.6}$$

Where:

$I_{\max}$ = signal amplitude (A)

Ω = 2πf; where f = frequency (Hz)

T = time (s)

The response is then:

$$V = V_{\max} \sin \ \omega t - \varphi \tag{2.7}$$

Where:

$V_{\max}$ = response amplitude

φ = phase angle

For a pure resistor, the phase angle φ =0, and the impedance Z=R

For a capacitor, the phase angle $\varphi = \frac{\pi}{2}$, and the impedance is:

$$Z_c = -\frac{j}{\omega C} \tag{2.8}$$

Where:

$j = \sqrt{-1}$

C = capacitance (F)

For a fuel cell equivalent circuit, such as the one shown in fig. 2-3, the impedances are:

$$Z_R = R_R; \quad Z_{act} = R_{act}; \quad Z_c = -\frac{j}{\omega C} \tag{2.9}$$

The impedance of the entire circuit is then:

$$Z\ \omega = R_R + \frac{1}{\frac{1}{R_{act}} - \frac{\omega C}{j}} = R_R + \frac{R_{act}}{1 + j\omega C R_{act}} \tag{2.10}$$

After rearranging, it becomes a complex number:

$$Z\ \omega = R_R + \frac{R_{act}}{1 + \ \omega C R_{act}^{\ 2}} - j\frac{\omega C R_{act}^{\ 2}}{1 + \ \omega C R_{act}^{\ 2}} \tag{2.11}$$

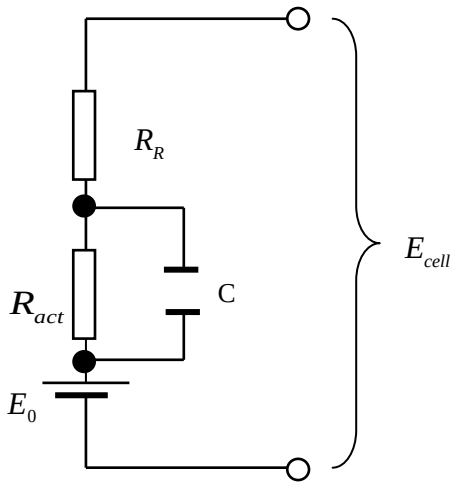

Equivalent circuit model of a Fuel Cell

Figure 2-3: Equivalent circuit representing a fuel cell

with the real part:

$$\mathrm{Re}\, Z = R_R + \frac{R_{act}}{1 + \ \omega C R_{act}^{\ 2}} \tag{2.12}$$

and the imaginary part:

$$\mathrm{Im}\, Z = \frac{\omega C R_{act}^{\ 2}}{1 + \ \omega C R_{act}^{\ 2}} \tag{2.13}$$

Where,

R_R = Ohmic Resistance

R_{act} = Activation Resistance

With the absolute value of the impedance:

$$|Z| = \left[\ \mathrm{Re}\, Z^{\ 2} + \ \mathrm{Im}\, Z^{\ 2} \right]^{\frac{1}{2}} \tag{2.14}$$

And the phase angle:

$$\tan \ \varphi = \frac{\mathrm{Im}\, Z}{\mathrm{Re}\, Z} \tag{2.15}$$

Plotted in a Nyquist Diagram (Im Z vs Re Z), the measurements of a complex impedance at various frequencies of this simple fuel cell equivalent circuit may result in a semicircle as seen in fig. 2-4. At very low frequencies, the resulting impedance is $Z = R_R + R_{act}$, whereas at high

frequencies, the resulting impedance is $Z = R_R$. Sometimes a single measurement at high frequency is used to measure the cell resistance R_R. However, the entire frequency spectrum may provide more useful information about the cells inner working [28].

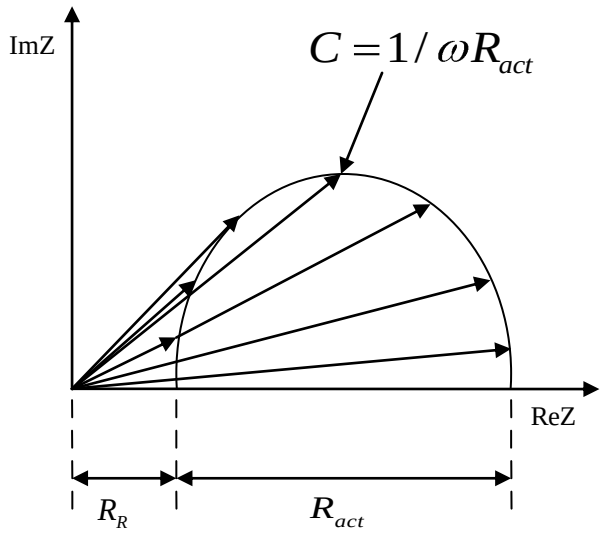

Figure 2-4: Resulting complex impedance at various frequencies of a fuel cell.

3. EXPERIMENTAL SET-UP:

3.1 Cell Preparation:

An 850e 50cm² active area fuel cell fixture consisting of gold plated current collectors, and aluminum end plates, from Scribner Associates Inc. (USA) was used for all experiments. A perfluorosulfonic acid (PFSA) catalyst coated membrane (Nafion® 212) from Lynntech Inc. was employed in the MEAs with 0.5mg/cm² and 1mg/cm² Pt/C catalyst loading respectively. The experimental set-up is as shown in Fig. 3-1. The Nafion catalyst coated membrane (CCM) was sandwiched between carbon cloth gas diffusion layers with hydrophobic layers to obtain a 50cm² active area MEA. Single cells were assembled using single serpentine flow field channels machined into poco graphite blocks. A Teflon gasket of thickness, 8µm, from BASF Fuel Cell inc., was used as sealant to prevent gas leakage. Each of the bolts on the fuel cell fixture was tightened to a required torque force of 90in/lb using a torque wrench so as to prevent gas leakage and back flow of reactant gas. A type T thermocouple was used as temperature sensor with a CSC32T temperature controller from Omega engineering Inc. to control the temperature of the PEM fuel cell. The thermocouple probe was inserted into the thermocouple well provided in the cathode side of the end plate and the plug connector on the thermocouple was connected to the temperature controller. This way the temperature controller can read and measure the temperature of the cell. It is assumed that the temperature at the cathode side of the end plate at any time is approximately equal to the temperature of the whole PEM fuel cell. The cartridge heater on the fuel cell was plugged into the temperature controller so as to heat the cell at a controlled temperature.

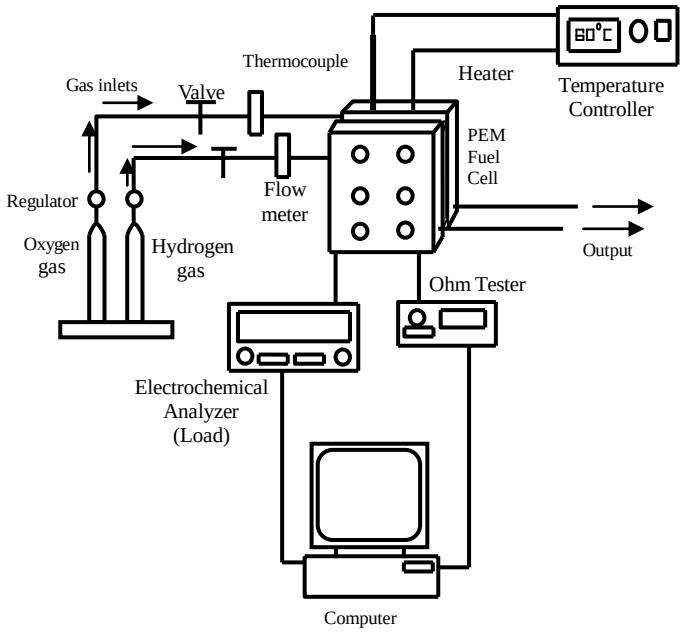

Figure 3-1. PEM Fuel Cell Experimental Set-up

3.2 Diagnostic Tests:

Diagnostic tests were performed during the experiments in order to determine fuel cell performance change. The duration of each test conducted was 24 hours. Hydrogen and pure oxygen were used as reactant gases. The reactant gas flow rates were controlled using a flow meter. The cell temperature was controlled at 60°C. The reactant flow pressure was kept at 30psi for both gases. Back pressure of the cell was maintained at ambient. The area specific resistance and cell voltage were measured using a high frequency (1 kHz) resistance meter (Model 3566, Tsuruga Electric, Japan). Tafel measurements were taken to measure the rate of the electrochemical reaction taking place at the electrodes, and, AC Impedance spectroscopy measurements were taken to measure cell performance using the CHI660B electrochemical analyzer. Dell computers fully installed with data acquisition software were used to collect data measured by the CHI660B and Tsuruga Electric resistance meter.

3.3 Experimental Procedure:

The PEM Fuel Cell performance test was run with two (2) factors each at two (2) levels. The two factors are the catalyst loading of the MEA and the flow rate of the reactant gases (Hydrogen and Oxygen), and the two levels are the high and low levels of each of the two factors, i.e. 0.5mg/cm² and 1mg/cm² catalyst loading are the same at the anode and cathode side, and 0.3L/min and 0.5L/min reactant gas flow rate are the same for hydrogen and pure oxygen gas. There were four test runs to investigate the effects of the two factors at each levels, and for every test combination, a new MEA was used; MEA with 0.5mg/cm² catalyst loading, same for the anode and cathode sides, and 0.3L/min reactant gas flow rate, same for both hydrogen and pure oxygen gas, 1mg/cm² catalyst loading, same for the anode and cathode sides, and 0.3L/min gas flow rate, same for both hydrogen and oxygen gas, 0.5mg/cm² catalyst loading, same for the anode and cathode sides, and 0.5L/min gas flow rate, same for both hydrogen and oxygen gas, and 1mg/cm² catalyst loading, same for the anode and cathode sides, and 0.5L/min, same for both hydrogen and oxygen gas. As observed in numerous literatures, the gas flow rate used to test fuel cells of 25cm² and 50cm² active area ranges from 0.1L/min to 0.5L/min, and sometimes, 1L/min. The reactant gas flow rates of 0.3L/min and 0.5L/min were selected based on the range of gas flow rates used in literature to understand the relationship between gas flow rate and fuel cell performance and degradation. The Scribner associates fuel cell fixture was assembled with each MEA for each test run. The Fuel cell was controlled at a steady temperature of 60°C and ambient pressure for each run. The oxygen and hydrogen gases were fed into the cell without humidification. To stabilize the fuel cell, it was left to run without taking readings for 2 hours. After 2 hours of operation, for each of the four test runs, performance tests were conducted where the fuel cell was run for 24hrs, during which electrochemical tests were performed at intervals as described in the respective methods in the following sections. The parameters measured with the CHI660B instrument and AC ohm tester are:

1. Tafel Plot
2. AC impedance
3. Area specific resistance
4. Open circuit voltage

Polarization (I/V) curve measurements were not taken as we had limited options of measurement techniques of the equipment used for electrochemical testing. Communication between the CHI600B Electrochemical Analyzer and the data acquisition device (computer) is through an RS-232 serial port via a 9F-25M serial cable. The Com Port 25-pin connector at the rear panel of the CHI660B was connected to the 'COM1' serial port of the computer, and the data acquisition software for the CHI660B was installed in the computer.

4. EXPERIMENTAL RESULTS AND DISCUSSIONS:

4.1 AC Impedance/EIS:

EIS was applied to study the performance degradation of the PEM Fuel Cell [4]. The CHI660B was used to measure the AC impedance of the PEM Fuel Cell for the four test runs. The test frequency scope was from 1Hz to 10 kHz, and the simulated amplitude was 0.005V. The AC Impedance measurements for each of the test runs were taken after 20hrs of cell operation. On the data acquisition software window, the technique command was selected and AC Impedance technique was chosen to run. The parameter settings for the AC impedance technique are as shown below:

Initial E (V): 0
High frequency (Hz): 10000
Low frequency (Hz): 1
Amplitude (V): 0.005
Quiet time (s): 2
Sensitivity: Automatic

The frequency is scanned from the selected high frequency to the selected low frequency. The current and potential are sampled and analyzed to obtain the real and imaginary impedance.

AC Impedance diagrams were simulated using an equivalent circuit in Fig. 2-3. Figure 4-1 shows the AC Impedance Nyquist plots obtained for MEA's with 0.5mg/cm² and 1mg/cm² catalyst loading tested at a flow rate of 0.3L/min. It is observed that the MEA with a higher catalyst loading of 1mg/cm² has a higher activation resistance and lower ohmic resistance than the MEA with low (0.5mg/cm²) catalyst loading. But both MEAs show the same total fuel cell resistance. Figure 4-2 also shows Nyquist plots of MEAs with 0.5mg/cm² and 1mg/cm² catalyst loading tested at a higher flow rate of 0.5L/min. It is observed here that the MEA with 0.5mg/cm² catalyst loading tested at 0.5L/min has the highest activation resistance, therefore has the highest resistance to charge transfer for oxygen reduction reaction, but both loadings gave the same ohmic resistance. MEA with 0.5mg/cm² (low) catalyst loading tested at lower flow rate (0.3L/min) gave a lower ohmic and activation resistance (1.48 and 0.62 Ω respectively) compared to MEA with same catalyst loading tested at higher flow rate (0.5L/min) which gave the highest ohmic and activation resistance of 3 and 115 Ω respectively. This shows an increase in total cell resistance, which implies that ion conductivity decreases at higher flow rate. The MEA with 0.5mg/cm² catalyst loading tested at 0.3L/min flow rate gave the best performance as it has a low activation, and ohmic resistance, followed by the MEA with 1mg/cm² catalyst loading tested at 0.3L/min gas flow rate. In summary, with the increase of catalyst loading from 0.5mg/cm² to 1mg/cm² at low flow rate (0.3L/min), the ohmic resistance slightly decreased and activation resistance slightly increased but total fuel cell resistance remains the same. But at the higher flow rate (0.5L/min), there is a significant decrease of total resistance, and activation resistance, but ohmic

resistance remains the same.The AC Impedance values as seen in the graph are summarized in Table 1.

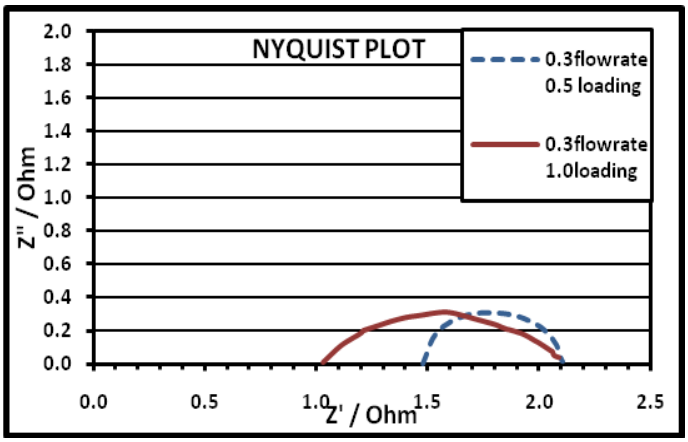

Figure 4-1: Nyquist Plot of Fuel cell with MEAs of 0.5mg/cm² and 1mg/cm² operated at gas flow rates of 0.3L/min.

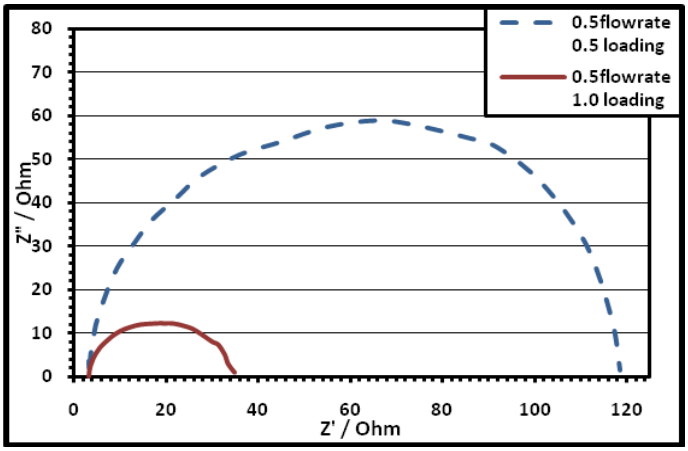

Figure 4-2: Nyquist Plot of Fuel cell with MEAs of 0.5mg/cm² and 1mg/cm² operated at gas flow rates of 0.5L/min.

TABLE SHOWING AC IMPEDANCE (ohms) VALUES OF EACH MEA AT DIFFERENT FLOWRATES						
	MEA CATALYST LOADING					
	0.5mg/cm²			1mg/cm²		
Flowrates	R(Ohmic)	R(act)	Total R	R(ohmic)	R(act)	Total R
0.3L/min	1.48	0.62	2.1	1.02	1.08	2.1
0.5L/min	3	115	118	3	33	36

Table 1: Impedance values of MEA at different reactant gas flow rates

4.2 Tafel Plot:

The CHI660B was used to take Tafel measurements. The Tafel measurement was taken after 22hrs of fuel cell operation for each of the four test runs. On the data acquisition software window, the technique command was selected and Tafel technique was chosen to run. The parameter settings for Tafel technique are as follows:
Initial E (V): 0; Final E (V): 1; Sweep segment: 1;
Hold time at final E: 0; Scan rate: 0.00333; Quiet time (s): 2;
Sensitivity: $1\,e^{-001}$

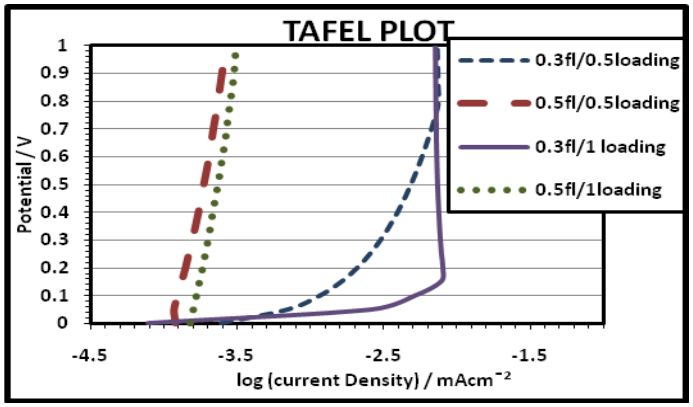

Figure 4-3: Tafel Plot for MEA loading and gas flow rate combinations.

The results of the Tafel plot is shown in figure 4-3. It can be seen from Fig. 4-3 that the MEA with 0.5mg/cm² catalyst loading tested at reactant gas flow rate of 0.3L/min has the highest exchange current density value of -2.05 mAcm², therefore it had the least activation loss and faster reaction rate, while the MEA with 0.5mg/cm² catalyst loading tested at a reactant gas flow rate of 0.5L/min had the least exchange current density value of -3.9 mAcm², therefore had the highest activation loss and slowest reaction rate. This result as observed in the Tafel plot agree with the ac impedance results, that the MEA with catalyst loading of 0.5mg/cm² tested at 0.3L/min gas flow rate performed best followed by MEA with 1mg/cm² catalyst loading tested at 0.3L/min gas flow rate. It can also be seen that the MEA with 1mg/cm² catalyst loading tested at 0.5L/min flow rate has the next higher activation loss and slower reaction rate. These results based on Tafel agree with the results based on AC Impedance Nyquist plot. The exchange current density values of all the MEAs are summarized in Table 2.

Table showing exchange current density value (mA/cm²) from Tafel plot		
	MEA CATALYST LOADING	
Flowrates	0.5mg/cm²	1mg/cm²
0.3L/min	-2.05	-2.2
0.5L/min	-3.9	-3.8

Table 2: Exchange current density values of MEA at different loading and flow rate.

4.3 Open Circuit Voltage – Time plot:

The open circuit voltage – time graph shows the output voltage performance of the fuel cell. The readings of the four experiments conducted were taken using Tsuruga Electric Ohm tester Model no. 3566 at two hour intervals during the course of each 24 hour experiment. From Fig. 4-4 and Table 3, it is observed that the OCV curve for all the MEAs decreased gradually with time. This pattern agrees with published literature [29].

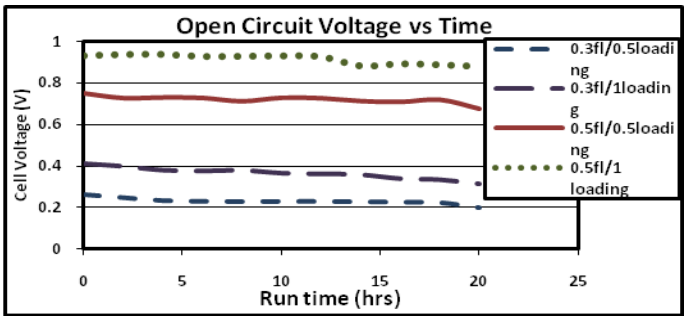

Figure 4-4. Open Circuit Voltage-Time graph

Open Circuit Voltage (V) of Fuel Cell easured at 2 hour intervals using Tsuruga Electric Ohm tester			
0.5mg/cm² Catalyst Loading		1mg/cm² Catalyst Loading	
0.3L/min gas flow rate	0.5L/min gas flow rate	0.3L/min gas flow rate	0.5L/min gas flow rate
0.2652	0.7468	0.4133	0.9297
0.2498	0.7241	0.4001	0.9355
0.2343	0.7271	0.3805	0.9362
0.2311	0.7247	0.3766	0.9261
0.2294	0.7088	0.3798	0.9273
0.2305	0.7257	0.3657	0.9288
0.2301	0.7233	0.3621	0.9254
0.2286	0.7097	0.3578	0.8824
0.2265	0.7055	0.3381	0.8922
0.2239	0.7164	0.3329	0.8879
0.1978	0.6725	0.3116	0.8802

Table 3: OCV measurements taken using the Tsuruga Electric Ohm Tester.

The MEA with catalyst loading of 0.5mg/cm² tested at reactant gas flow rates of 0.3L/min show the most OCV decay with respect to time, and worst initial voltage of 0.2652 V and decay rate of 25.4%, followed by MEA with catalyst loading of 1mg/cm² tested at 0.3L/min flow rate, which had the next lowest output voltage of 0.4133 V and decay rate of 24.6%. The best performing MEA in terms of decay and output voltage was MEA with catalyst loading of 1mg/cm² tested at 0.5L/min flow rate, giving an initial voltage of 0.9297 V, and decay rate of 5.3%, followed by MEA with 0.5mg/cm² catalyst loading tested at 0.5L/min gas flow rate giving an initial voltage of 0.7468, and decay rate of 9.95%. The theoretical OCV which is the difference between the equilibrium potentials of hydrogen oxidation reaction (HOR) and oxygen oxidation reaction (ORR) usually deviates from its 1.23V value under normal operating conditions. The decay of the OCV observed in each of the four experiments run can be considered to originate from increase in hydrogen crossover, dissolution/corrosion of Pt catalyst and carbon support, and decay of oxygen reduction reaction (ORR) kinetics or loss of ORR activity [29].

4.4 Area Specific Resistance:

When referring to Area Specific Resistance it must be clear as to what is causing the resistance. The measured Area Specific Resistance is dominated by the membrane in a fuel cell; this is the result of the resistance introduced by other fuel cell components and interfaces. Area Specific Resistance is calculated by multiplying the Area times the measured resistance in a fuel cell. It is measured in Ω cm² and shows the effects of resistance of each active area on the cell performance. Figures 4-5 and 4-6 shows the area specific resistance measured of each MEA. It is observed that MEA with 1mg/cm² catalyst loading tested at 0.3L/min reactant gas flow rate had the least resistance while both catalysts loaded MEA's operated at 0.5L/min reactant gas flow rate exhibited the high resistance. This shows the effect of reactant gas flow rate on cell performance.

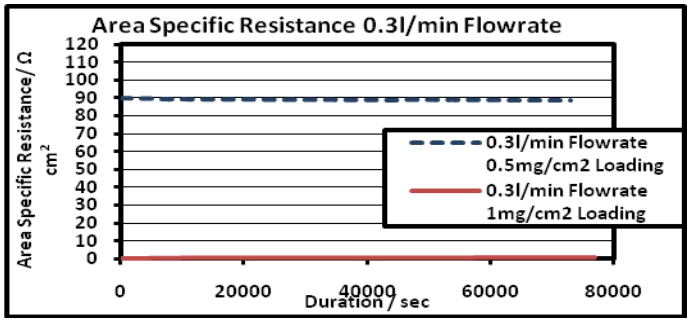

Figure 4-5. Area specific resistance plot of 0.5mg/cm² and 1mg/cm² catalyst Loading MEA at 0.3L/min gas flow rate.

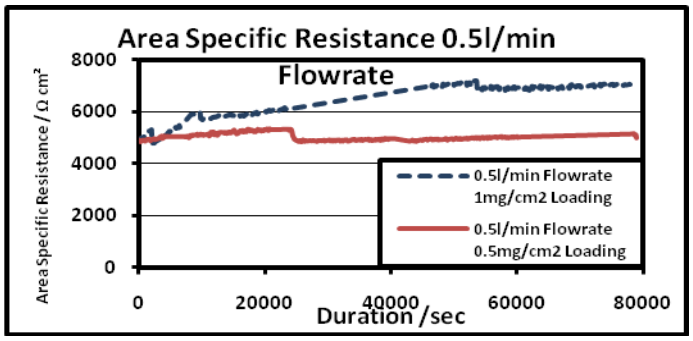

Figure 4-6. Area specific resistance plot of 0.5mg/cm² and 1mg/cm² catalyst loading MEA at 0.5L/min gas flow rate.

5. CONCLUSION

From the results of this research, the following conclusions could be made:

1. Process parameters – catalyst loading and gas flow rate have significant effect on PEM Fuel Cell performance.
2. MEAs with lower gas flow rate of 0.3L/min has lower ohmic resistance, activation resistance, and total cell resistance, than MEAs with higher gas flow rate of 0.5l/min.
3. MEAs with higher catalyst loading of $1mg/cm^2$ has lower ohmic resistance, activation resistance, and total cell resistance than MEAs with lower catalyst loading of $0.5mg/cm^2$.
4. The best performing MEA observed from AC Impedance/ EIS was the MEA with catalyst loading of $1mg/cm^2$ tested at gas flow rate of 0.3L/min, which gave an ohmic resistance of 1.02 Ω, an activation resistance of 1.08 Ω, and a total cell resistance of 2.1 Ω.
5. TAFEL plot shows the highest exchange current density value of -2.05 $mAcm^2$ for MEA with $0.5mg/cm^2$ catalyst loading tested at reactant gas flow rate of 0.3L/min signifying that it has the least activation loss and fastest reaction rate, followed by MEA with $1mg/cm^2$ catalyst loading and 0.3L/min flow rate, having the next fastest reaction rate.
6. TAFEL plot also shows the lowest exchange current density value of -3.9$mAcm^2$ for MEA with $0.5mg/cm^2$ catalyst loading tested at a gas flow rate 0.5L/min, followed by MEA with $1mg/cm^2$ catalyst loading tested at a gas flow rate of 0.5L/min.
7. The Open Circuit Voltage-Time measurements taken show that the MEAs tested at higher gas flow rate of 0.5L/min give a higher output voltage than MEAs tested at lower reactant gas flow rate of 0.3L/min, which implies that higher catalyst loading and higher gas flow rate produces higher output voltage, therefore output voltage increases with increase in catalyst loading and gas flow rate.
8. It was hypothesized that the cause of the degradation in the OCV of each of the MEAs was as a result of voltage losses from activation and ohmic resistance as observed in TAFEL and AC Impedance mesurements.
9. Increasing the catalyst loading and decreasing the gas flow rate will reduce activation loss and improve PEM Fuel Cell performance.
10. For our future work, the effects of other operating parameters, such as, temperature, relative humidity, MEA thickness, hydrogen crossover, radical attack, etc., which affect PEM Fuel Cell performance and durability will be investigated for improvement. Novel bipolar plate materials which have been identified for improved PEM Fuel Cell performance will be tested with identified high performance MEAs, and compared with conventional MEAs and bipolar plate materials.

Acknowledgements:

The authors would like to thank Dr. Peixin He of CH Instruments inc. for the loan of CHI660B instrument that was used for this research, Dr. Tsu of BASF Fuel Cell inc. for the donation of Teflon materials used as sealant, and Jason Scribner of Scribner Associates inc. for valuable discussions and cooperation. The Graduate Research Assistantship from Dr. A. C. Okafor, and the Intelligent Systems Center is gratefully acknowledged. The Graduate Teaching Assistantship from the Department of Mechanical and Aerospace Engineering at the Missouri University of Science and Technology is also gratefully acknowledged.

References

[1] Freya, Th., and Linardi, M., 2004, "Effects of membrane electrode assembly preparation on the polymer electrolyte membrane fuel cell performance", Electrochim. Acta, 50, pp. 99–105.

[2] Vogel, B., Aleksandrova, E., Mitov, S., Krafft, M., Dreizler, A., Kerres, J., Hein, M., and Rodunera, E., 2008, "Observation of Fuel Cell Membrane Degradation by Ex Situ and In Situ Electron Paramagnetic Resonance", J. Electrochem. Soc. 155 (6) B570-B574.

[3] Mittal, V. O., Kunz, H. R., and Fenton, J. M., "Degradation mechanisms in PEMFCs", 2007, J. Electrochem. Soc. 154(7), B652-B656.

[4] Schulze, M., Wagner, N., Kaz, T., and Friedrich, K.A., 2007, "Combined electrochemical and surface analysis investigation of degradation processes in polymer electrolyte membrane fuel cells", Electrochim. Acta, 52, pp. 2328–2336.

[5] Alink, R., Gerteison, D., and Oszcipok, M., 2008, "Degradation effects in polymer electrolyte membrane fuel cell stacks by sub-zero operation – An in situ and ex situ analysis", J. Power Sources 182, pp. 175-187.

[6] Wolfgang S., and Ardalan V., 2008, "A review of the main parameters influencing long-term performance and durability of PEM fuel cells", J. Power Sources 180, pp. 1–14.

[7] Schulze, M., Knori, T., Schneider, A., and Gulzow, E., 2004, "Degradation of sealings for PEFC test cells during fuel cell operation", J. Power Sources 127, pp. 222 -229.

[8] Ahn, S.Y., Shin, S.-J., Ha, H.Y., Hong, S.A., Lee, Y.C., Lim, T.W., and Oh, I.H., 2002, "Performance and lifetime analysis of the kW-class PEMFC stack", J. Power Sources 106, pp. 295-303.

[9] Ma, L., Wartgesen, S., and Shores, D.A., 2000, "Evaluation of materials for bipolar plates in PEMFCs" J. New Mat. Electrochem. Syst. 3, pp. 221-228.

[10] Taniguchi, A. Akita, T., Yasuda, K., Miyazaki, Y., 2004, "Analysis of electrocatalyst degradation in PEMFC caused by cell reversal during fuel starvation", J. Power Sources 130, pp. 42-49.

[11] Yu, J., Matsuura, T., Yoshikawa, Y., Islam, M.N., and Hori, M., 2005, "In Situ analysis of performance degradation of a PEMFC under non saturated humidification", Electrochem. Solid State Lett. 8, A156-A158.

[12] Yu, J., Yi, B., Xing, D., Liu, F., Shao, Z., Fu, Y., and Zhang, H., 2003, "Degradation mechanism of polystyrene sulfonic acid membrane and application of its composite membranes in fuel cells", Phys. Chem. Chem. Phys. 5, pp. 611-615.

[13] Knights, S.D., Colbow, K.M., St-Pierre, J., Wilkinson, D.P., 2004, "Aging mechanisms and lifetime of PEFC and DMFC", J. Power Sources 127, pp. 127-134.

[14] St-Pierre, J., Wilkinson, D.P., Knights, S., and, Bos, M.L., "Relationships between water management, contamination and lifetime degradation in PEFC", 2009, J. New Mat. Electrochem. Syst. 3, pp. 99-106.

[15] Kundu, S., Fowler, M.W., Simon, L.C., and, Grot, S., 2006, "Morphological features (defects) in fuel cell membrane electrode assemblies", J. Power Sources 157, pp. 650–656.

[16] Xingwen Y., and, Siyu Y., 2007, "Recent advances in activity and durability enhancement of Pt/C catalytic cathode in PEMFC Part II: Degradation mechanism and durability enhancement of carbon supported platinum catalyst", J. Power Sources 172, pp. 145–154.

[17] Jinfeng W., Xiao Z.Y., Jonathan J. M., Haijiang W., Jiujun Z., Jun S., Shaoshong W., and Walter M., 2007, " A review of PEM fuel cell durability: Degradation mechanisms and mitigation strategies", J. Power Sources 184, pp. 104-119.

[18] Thanganathan U., and Masayuki N., 2007, "Characterization and performance Improvement of H_2O_2 Fuel Cells based on glass membranes". J. Electrochem. Soc. 154 (8) B845-B851.

[19] Hommura, S., Kawahara, K., Shimohira, T., and Teraoka, Y., 2008, "Development of a Method for Clarifying the Perfluorosulfonated Membrane Degradation Mechanism in a Fuel Cell Environment", J. Electrochem. Soc. 155 (1) A29-A33.

[20] Vogel, B., Aleksandrova, E., Mitov, S., Krafft, M., Dreizler, A., Kerres, J., Hein, M., and Rodunera E., 2008, "Observation of Fuel Cell Membrane Degradation by Ex Situ and In Situ Electron Paramagnetic Resonance", J. Electrochem. Soc. 155 (6). B570-B574.

[21] Yousfi, S. N., Mocoteguy, Ph., Candusso, D., Hissel, D. Hernandez, A., Aslanides, A., 2008, "A review on PEM voltage degradation associated with water management: Impacts, influent factors and characterization", J. Power Sources 183, pp. 260–274.

[22] Jinfeng, W., Xiao, Z. Y., Haijiang, W., Mauricio B., Jonathan J. M., Jiujun Z., 2008, "Diagnostic tools in PEM fuel cell research: Part I Electrochemical techniques", Int. J. Hydrogen Energy 33, pp. 1735– 1746.

[23] Parthasarathy, A., Dave, B., Srinivasan, S., and, Appleby, A., 1992, "The platinum microelectrode/Nafion interface: an electrochemical impedance spectroscopic analysis of oxygen reduction kinetics and Nafion characteristics", J. Electrochem Soc. 139 (6) pp. 1634–41.

[24] Springer, T., Zawodzinski, T., Wilson, M., Gottesfeld, S., 1996, "Characterization of polymer electrolyte fuel cells using AC impedance spectroscopy", J. Electrochem. Soc. 143 (2) 587-599.

[25] Romero, C. T., Arriaga, L., and Cano, C. U., 2003, "Impedance spectroscopy as a tool in the evaluation of MEAs", J. Power Sources 118(1–2) pp. 179–82.

[26] Song, J. M., Cha, S.Y., Lee, W. M., 2001, "Optimal composition of polymer electrolyte fuel cell electrodes determined by the AC impedance method", J. Power Sources 94 (1) pp. 78–84.

[27] James, L., and, Andrew, D., Fuel Cell systems explained, Second edition, Wiley Books, pp. 45-47

[28] Frano, B., "PEM Fuel Cells Theory and practice", Elsevir Academic Press, pp. 254-258

[29] Sugawara, S., Maruyama, T., Nagahara, Y., Kocha, S. S., Shinohra, K., Tsujita, K., Mitsushima, S., and Ota, K., 2009, "Performance decay of proton-exchange membrane fuel cells under open circuit conditions induced by membrane decomposition", J. Power Sources 187 (2) 324-331.